WPDC-CPR(17) 17252

R Luis et al.

Nuclear and Thermal Analysis of a Reflectometry Diagnostics Concept for DEMO

Preprint of Paper to be submitted for publication in Proceeding of
27th IEEE Symposium On Fusion Engineering (SOFE)

This work has been carried out within the framework of the EUROfusion Consortium and has received funding from the Euratom research and training programme 2014-2018 under grant agreement No 633053. The views and opinions expressed herein do not necessarily reflect those of the European Commission.

Nuclear and Thermal Analysis of a Reflectometry Diagnostics Concept for DEMO

R. Luís, R. Moutinho, L. Prior, P. B. Quental, A. Lopes, H. Policarpo,
N. Velez, A. Vale, A. Silva, A. Malaquias

***Abstract*— The reflectometry diagnostic (RF) for DEMO is envisaged to provide the electron density profile and to be used as a control diagnostic for the real-time vertical position controller. An initial conceptual study has been performed defining the position of the antennas and the routing of the waveguides. In the present design, the integration has been driven by the remote handling and blanket interfaces. To progress with the system integration, neutronics simulations were performed to assess the cooling requirements. This paper presents a nuclear and thermal analysis for the initial design of the reflectometry diagnostic for DEMO. The neutronics simulations were performed using the Monte Carlo simulation program MCNP6 and FENDL 2.1 cross-sections, while ANSYS Mechanical v18 was used to perform the thermal analysis. Simulation results show that the nuclear heat loads reach 8 W/cm^3 at the surface of the diagnostics section. Without an active cooling system, the operating temperatures of the components under such heat loads would be well above the acceptable from the thermo-mechanical point of view. The thermal analysis here presented provides the temperature distribution in the components when subjected to neutron/gamma irradiation and thermal radiation from the plasma, after the implementation of a preliminary design of the active cooling system. The operation temperatures of the plasma-facing antennas, as well as the performance of the diagnostics system from the neutron shielding point of view, are analysed and discussed in this paper.**

***Index Terms*—Diagnostics, DEMO, neutronics, reflectometry, slim cassette concept, thermal analysis**

I. Introduction

Among the viable candidates to be used as diagnostics in the future tokamak demonstration fusion reactor (DEMO), reflectometry systems are known for their reliability and long-term durability under neutron and gamma irradiation. The absence of front-end elements such as mirrors and sensors makes reflectometry systems especially suitable to withstand the harsh radiation environment foreseen for DEMO, during the extended periods of operation between blanket replacement. An innovative concept, involving the integration of several groups of antennas and waveguides into a full poloidal section of the Helium Cooled Liquid Lead (HCLL) breading blanket, is currently under study. Such a poloidal section, fully dedicated to diagnostics, must be seamlessly integrated in the blanket structure, conforming to the blanket cooling services and exhibiting similar thermo-mechanical behavior and neutron shielding performance as the full blanket segment. To fulfill the diagnostics requirements, it is anticipated that more than 100 antennas will be required, distributed in a few poloidal sections at several toroidal locations.

Fig. 1 shows a CAD representation of the Slim Cassette (SC) concept, a preliminary design of the diagnostics section featuring 40 antennas and corresponding waveguides, which are routed through the modules of the SC up to the diagnostics hall. As shown in Fig. 1 b), the antennas face the plasma directly, and are therefore exposed to high radiation doses, from plasma neutrons and from gamma photons generated in nuclear interactions in surrounding materials. Without an active cooling system, the operating temperatures of the components under such heat loads would be well above the acceptable from the thermo-mechanical point of view.

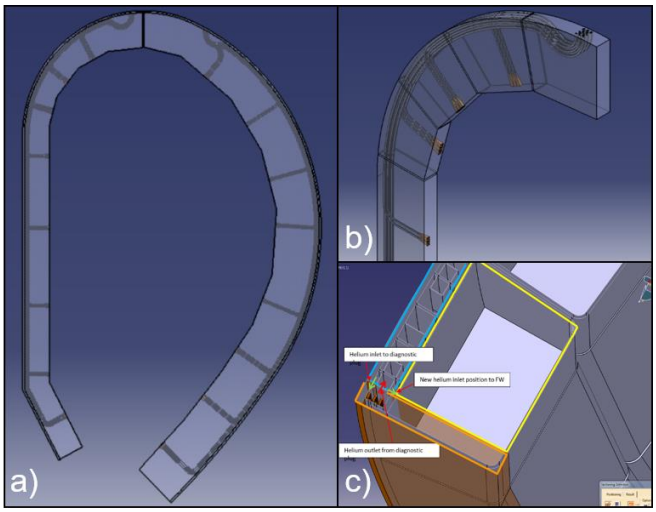

Fig. 1. a) Poloidal view of the Slim Cassette (SC). b) Detail showing the antennas and the waveguides inside the SC. c) Possible integration of the SC on the side of a blanket module.

This paper presents the results of a nuclear and thermal analysis performed for the currently proposed design of the SC, using MCNP6 and ANSYS Mechanical v18. A previous

Manuscript submitted on June 30th 2017. This work has been carried out within the framework of the EUROfusion Consortium and has received funding from the Euratom research and training programme 2014-2018 under grant agreement No. 633053. The reviews and opinions expressed herein do not necessarily reflect those of the European Commission.

R. Luís, R. Moutinho, L. Prior, P. B. Quental, A. Lopes, H. Policarpo, N. Velez, A. Vale, A. Silva and A. Malaquias are with the Instituto de Plasmas e Fusão Nuclear, Instituto Superior Técnico, Universidade de Lisboa, 1049 - 001 Lisboa, Portugal (e -mail: rluis@ipfn.tecnico.ulisboa.pt).

analysis had shown that the highest heat loads in the antennas are obtained at the equatorial level, in sectors 3-4 (inboard) and 10-13 (outboard) of Fig. 2. For this reason, the cooling system studied in this work was designed for one of the modules at the inboard side, to facilitate the design process and the implementation of the simulation models. The analyses presented in this paper refer to this module, described in section III.

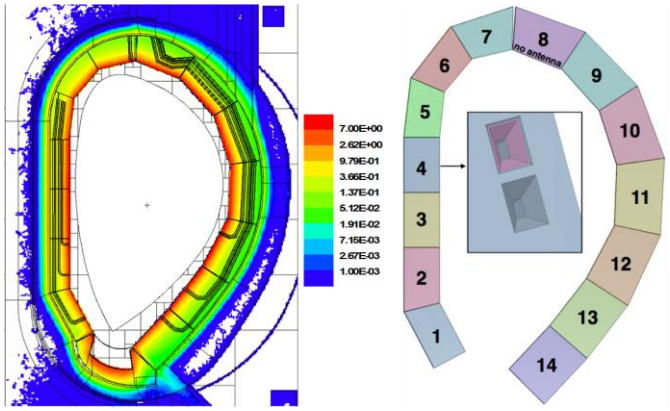

Fig. 2. Nuclear heat loads (W/cm^3) from a preliminary analysis. The heat loads are higher in the antennas of modules 3-4 and 10-13, i.e. closer to the equatorial plane.

II. Simulation Models and Tools

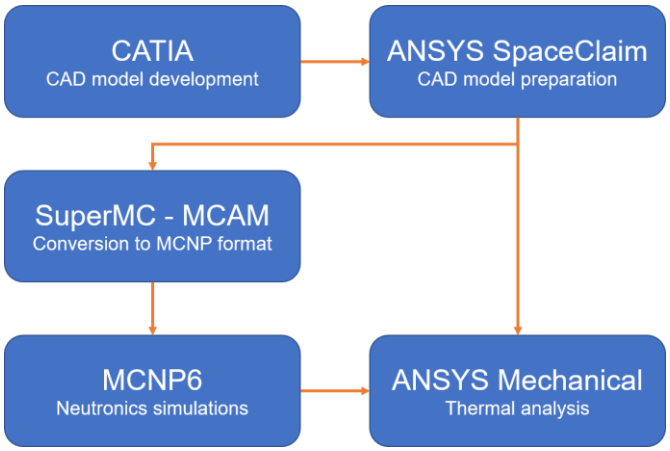

Fig. 3. Simulation tools used in the nuclear and thermal analyses.

Fig. 3 illustrates the steps followed to perform the simulations. The CAD software CATIA V5 [1] is used to develop the CAD models, which must be imported to ANSYS SpaceClaim [2] for simplification – removal of fillets, screws and other unnecessary complications – before they can be used in the nuclear and thermal analyses. For the nuclear analysis, the model is then exported as a STEP file and imported into the CAD-based modelling program MCAM [3,4] for conversion to the MCNP input format. The neutronics simulations are performed in the Monte Carlo simulation program MCNP6 [5], after the implementation of the converted model in a DEMO neutronics reference model, and the nuclear heat loads in the components of the SC are then used as input in ANSYS Mechanical v18 [2] to perform the finite element thermal analysis. The CAD models prepared in ANSYS SpaceClaim are used directly in the thermal analysis; there are only minor differences between the models used in the nuclear and thermal analyses, and these mostly related to the removal of spline surfaces that cannot be present in the model before conversion to MCNP.

A. CAD model

The CAD model of SC module studied in this paper is presented in Fig 4. Consecutive layers are shown from left to right:

- on the outside, the module is covered by a 2-mm tungsten layer;
- the first wall layer has a dedicated cooling system, with liquid helium entering the system at 300 ºC;
- inside, there are two vertical shielding segments, made of EUROFER;
- the antennas and the waveguides are sandwiched between the vertical shielding segments;
- each of the shielding segments has an active cooling system, as shown in the last frame.

Since helium leakage into the vessel is not allowed, the SC module uses a double containment barrier for helium, formed by the pipe loops (first barrier) and by the vertical plates, which are welded together (second barrier). In this first design, where the priority was the routing of the cooling system, only two antennas were introduced in SC module, to avoid unnecessary complications in the models.

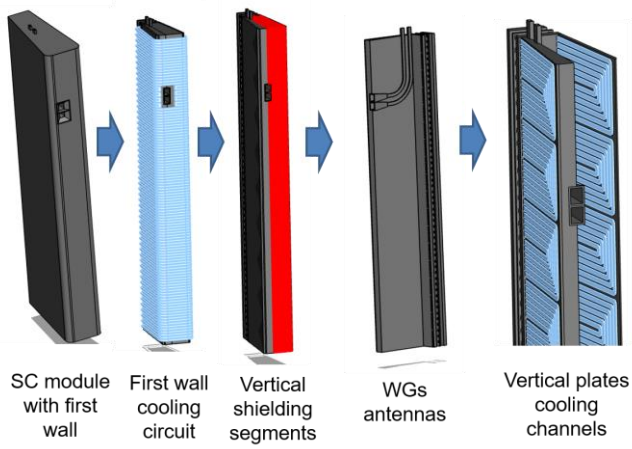

Fig. 4. CAD model of the SC module (inboard side), including two antennas and dedicated cooling systems.

B. MCNP model and simulation parameters

To perform the nuclear analysis, a DEMO MCNP reference model for the HCLL blanket configuration was used: 2015 DEMO HCLL MCNP model. This was originally a TRIPOLI model with empty blanket modules, which had been automatically converted to the MCNP input format; to have a usable reference model, some conversion errors present in the geometry were corrected and the blankets were filled with the homogeneous mixture detailed in Table 1, made of EUROFER (43.78% of the total volume), lithium lead (44.07%), tungsten (0.28%) and void (11.87%).

TABLE I
HCLL MODEL - MATERIAL SPECIFICATIONS FOR THE BLANKET MODULES

Radial Subdivision (%)	0.28%	3.46%	50.35%	0.00%	18.26%	27.66%	100.00%
Material	**Armour (2 mm)**	**FW (t=25 mm)**	**Breeding module**	**Caps**	**Back plates / Internal Manifolds**	**BSS**	**Vol. (%)**
Eurofer	0	71	16	78	58	82	**43.78**
PbLi (90% Li_6)	0	0	77	0	23	4	**44.07**
Tungsten	100	0	0	0	0	0	**0.28**
Void (Helium at 80 bar)	0	29	7	22	19	14	**11.87**
Total	100.0	100.0	100.0	100.0	100.0	100.0	**100.00**

The reference model with the SC module already implemented is shown in Fig. 5, for two perpendicular cuts. It represents a 10º toroidal sector of the DEMO reactor, with a 17 blanket module segmentation, corresponding to the present design of the HCLL blanket configuration. The SC module was implemented in the inboard side at the equatorial plane, in the blanket module of row #3, one of the locations with the highest thermal loads. It has a maximum width of 250 mm in the toroidal direction on the plasma-facing side and extends to the back of the blanket module in the radial direction.

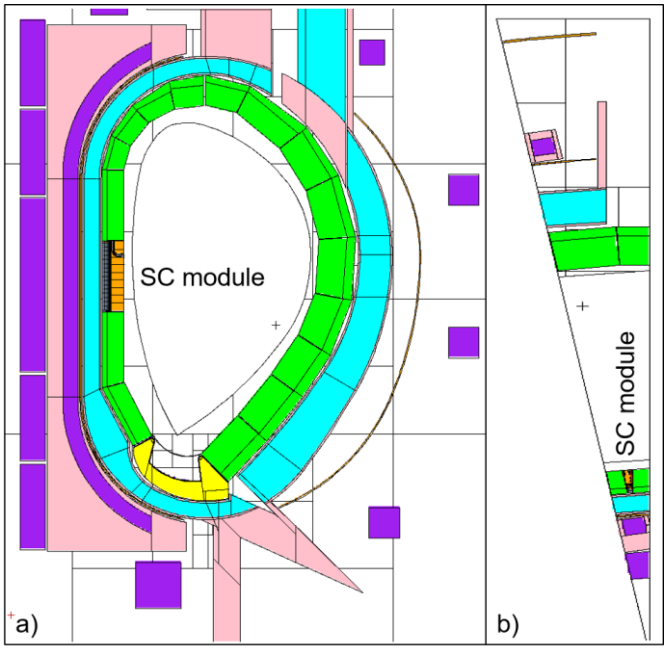

Fig. 5. DEMO HCLL reference MCNP model after implementation of the SC module. a) Poloidal plane. b) Toroidal plane (10º sector).

The MCNP model of the SC module is shown in more detail in Figs. 6 and 7, illustrating the complexity of the system, which, instead of homogeneous mixtures like the blanket modules, features all the elements of the cooling system implemented with the level of detail provided in the CAD drawings. The SC module, including the antennas and the waveguides, is mostly made of EUROFER, with two exceptions: the manifold, filled with a homogeneous material composition (also extracted from Table I), and the cooling pipes, filled with liquid helium at 80 bar.

The MCNP simulations were run using mode N P to simulate the transport of neutrons and photons, using an SDEF card with the particle weight set to 0.27778 to account for the fact that only a 10º sector is being modelled. FENDL 2.1 cross sections were used in the material definitions and the results were normalized to a fusion power of 2037 MW, according to the guidelines presented in [6]. To keep the statistical errors below 10% and to ensure that all tallies pass the 10 statistical tests of MCNP, 10^9 source particles were simulated in each run, using 400 processors of a Linux cluster (approximately 24 hours per run). F4 and F6 tallies were used to calculate fluxes and heat loads in the system, as well as mesh tallies of type 1 and 3. In particular, a very fine mesh with 640 000 bins (7.5 x 6.5 x 14.6 mm) was defined to calculate the nuclear heat loads in the SC module, to be used as input in the thermal simulations.

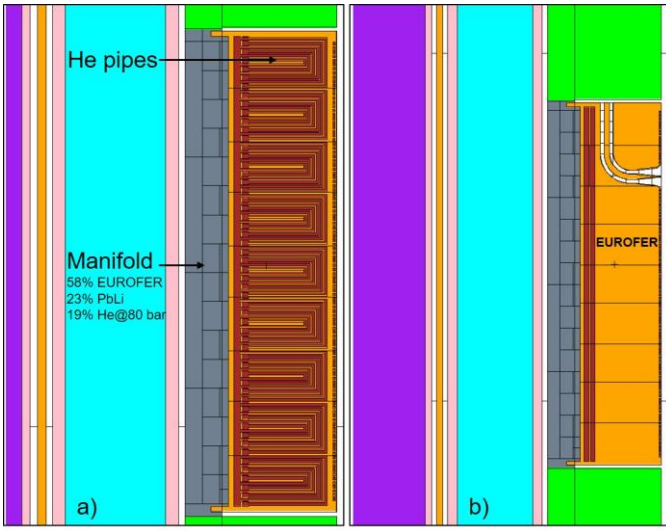

Fig. 6. Two poloidal cuts of the SC module, as implemented in MCNP.

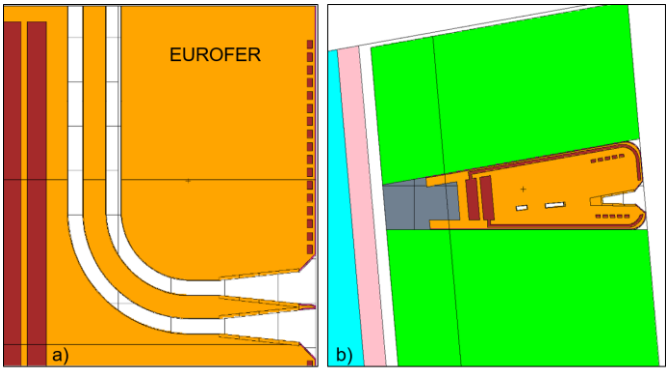

Fig. 7. SC module implemented in MCNP. a) Detail of the antennas and waveguides. b) Toroidal plane showing the different elements of the cooling system.

C. *Thermal simulation parameters*

As mentioned before, the CAD model prepared in ANSYS SpaceClaim (see Fig. 4) was used directly in the thermal analysis, without further modifications. The thermal radiation coming from the plasma was defined as surface-to-surface radiation, with a power density of 500 kW/m^2. Thermal fluid convection was defined for heat transport in the cooling channels, with a helium mass flow of 0.58 kg/s and a convection coefficient of 632 W/(m^2 K), entering the system at 300 ºC. Since the current design of the HCLL blanket modules foresees an inlet of helium at 300 ºC and an outlet at 500 ºC (the directions are reversed in consecutive pipes, to allow for an even heat distribution), an average temperature of 400 ºC was assumed at the interfaces with the blanket module. Finally, the nuclear heat loads calculated with MCNP were imported as internal heat generation, to account for the energy deposition by neutrons and photons in the SC module components.

III. Results and Discussion

A. *Nuclear analysis*

Figs. 8 and 9 show the neutron and photon fluxes in the system, respectively. The neutron fluxes reach 8x10^{14} neutrons/cm^2/s in the first wall of the SC module, while the gamma fluxes are lower: 1.5x10^{14} photons/cm^2/s. These flux meshes also show that no major issues related to neutron streaming are foreseen due to the introduction of the SC module, since the neutron fluxes behind the SC module are comparable with the fluxes behind the HCLL breeding blankets.

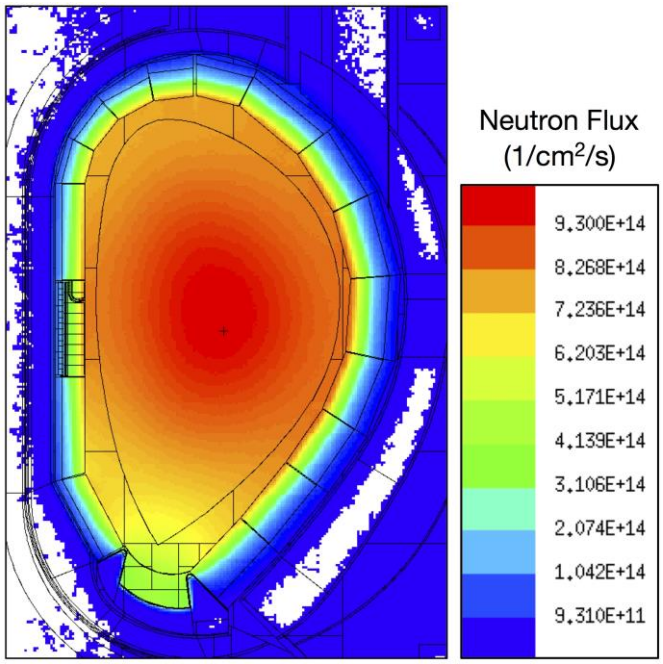

Fig. 8. Neutron fluxes (1/cm^2/s) in the whole model.

Fig. 9 also shows very clearly that the photon fluxes in the SC module are higher than fluxes in the breading blankets; this is due to the higher radiative capture cross sections of iron and chromium (the main constituents of EUROFER) when compared to the capture cross section of lead.

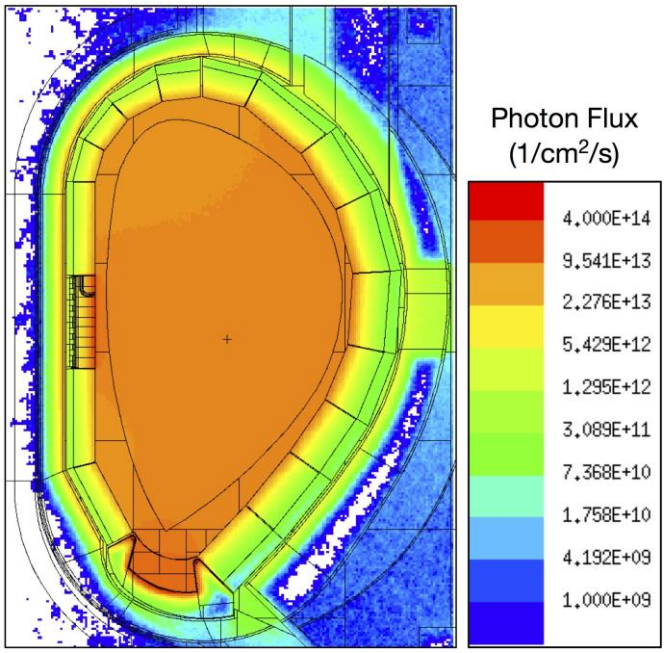

Fig. 9. Photon fluxes (1/cm^2/s) in the whole model.

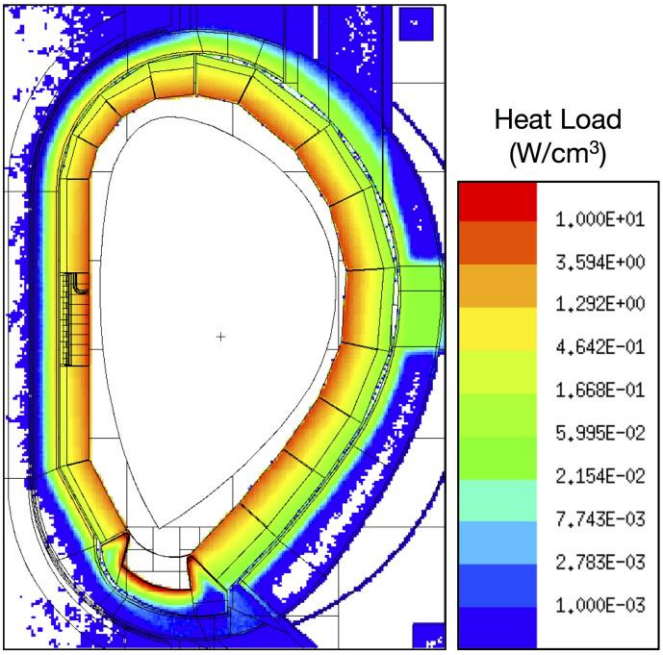

Fig. 10. Nuclear heat loads (W/cm^3) in the whole model.

The heat loads were also calculated, as shown in Figs. 10 (whole model) and 11 (SC module). Fig. 11 shows that the fine mesh employed in the heat load calculation is adequate in many regions to discriminate between the energy deposition in EUROFER and in the helium of the cooling pipes. Nevertheless, an even finer mesh would be preferable in some places, since some of the bins belong both to the cooling channels and to the shielding material, and the heat loads in those bins are averaged between the heat loads in adjacent components (this is the case in most of the small pipes of the cooling system). A finer mesh with 2.8 million bins was tested, but the statistics of the results were greatly affected, and the

output files became too heavy to be used as input in ANSYS Mechanical. The heat loads reach 8 W/cm^3 in the first wall of the SC, which will contribute to the high operation temperatures of the system, presented in the next section.

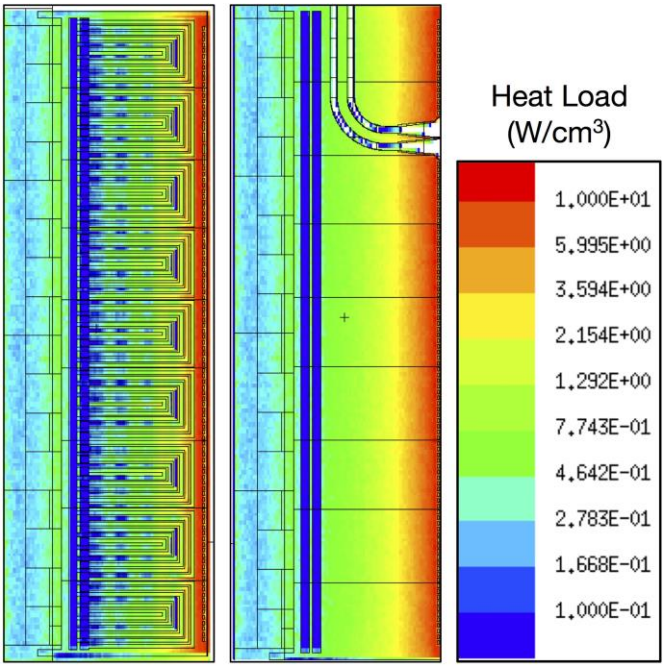

Fig. 11. Nuclear heat loads (W/cm^3) in the SC module.

The neutron and photon fluxes and the nuclear heat loads were also calculated separately in the antennas and waveguides. For these calculations, each of the two antenna systems was split into nine cells, as shown in Fig. 12: four cells in the antennas and five cells in the waveguides. The neutron and photon flux spectra in the four antenna cells of one of these systems (the results are similar in both) are shown in Fig. 13. As expected for a plasma-facing component, there is a sharp peak at 14 MeV for neutrons, which rises above most of the spectrum; the photon fluxes, on the other hand, are higher for energies between 100 keV and 10 MeV, with clearly defined peaks for energies up to 1 MeV.

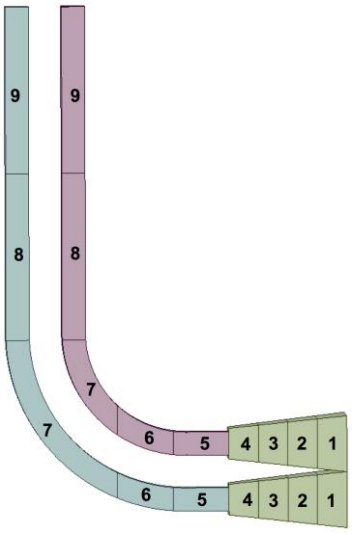

Fig. 12. Segmentation of the antennas and waveguides, used to calculate fluxes and heat loads.

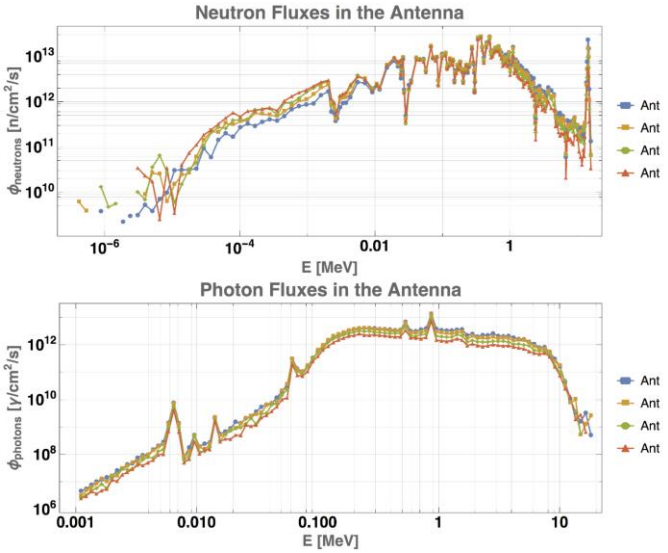

Fig. 13. Neutron and gamma fluxes (1/cm^2/s) in the four segments of one of the antennas.

The heat loads in each of these components are presented in Table 1, along with the statistical errors and the relative contributions from neutrons and photons to the total heat loads. Peak values of 7 W/cm^3 were obtained at the tips of the antennas, decreasing rapidly in subsequent cells as the distance to the plasma increases. As for the relative contribution from neutrons and photons, photons contribute the most to the total heat loads, an expected result since the antennas and waveguides are made of EUROFER. At the tips of the antennas, the contribution from photons to the total heat load is 75%, increasing up to 81% in subsequent cells. For visualisation purposes, the total heat loads in each of these cells are plotted in Fig. 14.

TABLE I
HEAT LOADS IN THE ANTENNAS AND WAVEGUIDES

System/ Component		#	Total Heat Load (W/cm^3)	Stat. Error (%)	Heat Load by Neutrons (%)	Heat Load by Photons (%)
Upper System	Ant. 1	1	7.06	0.6	25.3	74.7
	Ant. 2	2	5.69	0.7	22.0	78.0
	Ant. 3	3	4.36	0.9	20.4	79.6
	Ant. 4	4	3.26	1.2	19.7	80.3
	WG 1	5	2.22	1.6	19.9	80.1
	WG 2	6	1.39	2.0	19.9	80.1
	WG 3	7	0.98	1.9	19.0	81.0
	WG 4	8	0.87	1.5	19.6	80.4
	WG 5	9	0.76	1.5	22.4	77.6
Lower System	Ant. 1	1	7.03	0.6	25.2	74.8
	Ant. 2	2	5.73	0.7	21.9	78.1
	Ant. 3	3	4.36	0.9	20.5	79.5
	Ant. 4	4	3.24	1.2	19.8	80.2
	WG 1	5	2.16	1.6	19.8	80.2
	WG 2	6	1.46	1.9	18.8	81.2
	WG 3	7	0.79	1.4	19.7	80.3
	WG 4	8	0.51	1.7	20.6	79.4
	WG 5	9	0.57	1.7	23.2	76.8

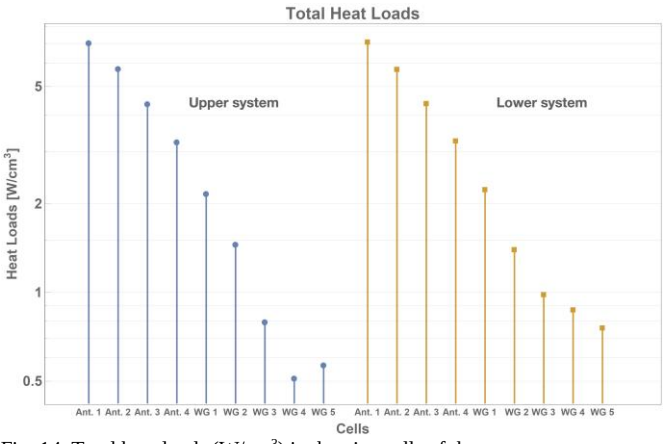

Fig. 14. Total heat loads (W/cm^3) in the nine cells of the two antenna systems.

B. *Thermal analysis*

The nuclear heat loads as imported from MCNP to ANSYS Mechanical are presented in Fig. 14. As before, we see peak values of the order of 8 W/cm^3 in the plasma-facing first wall. The thermal analysis was performed in steady-state conditions, using the radiosity solver. The thermal contact between surfaces was set as perfect. To simulate the heat transport in the cooling channels, the ANSYS element FLUID116 was used. The finite element model of these components has more than 5 million nodes, to account for the complexity of the geometry. The cooling channel heat transfer coefficient was calculated through the Dittus-Boetler correlation [7].

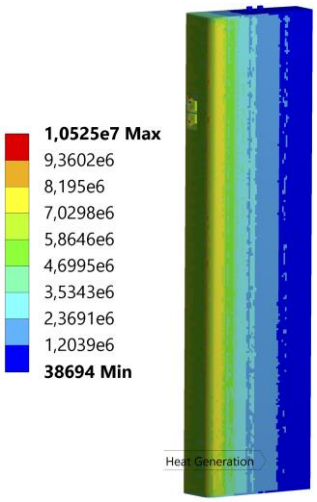

Fig. 14. Nuclear heat loads (W/m^3) as imported from MCNP into ANSYS Mechanical.

Taking into account the thermal radiation coming from the plasma, as well as the operation of the cooling system and the boundary conditions defined in section II, this translates into the operation temperatures shown in Fig. 15, for the first wall, cooling system, antennas and waveguides. There are very pronounced hotspots in some regions, most notably in the antennas, but also in the lower and upper parts of the system, where temperatures rise above 1100 ºC. These are mostly in elements located at larger distances from the cooling channels. Apart from these hotspots, the temperatures in the first wall reach approximately 700 ºC, decreasing rapidly for components located further away from the first wall. Increasing the helium flux by 50% in the cooling pipes yields only marginally better results, as shown in Fig. 16 (the maximum operation temperatures decrease by approximately 100 ºC). Overall, these results show that the design of the cooling system must be improved in order to increase the flow of helium near the antennas, as well as in the upper and lower parts of the system.

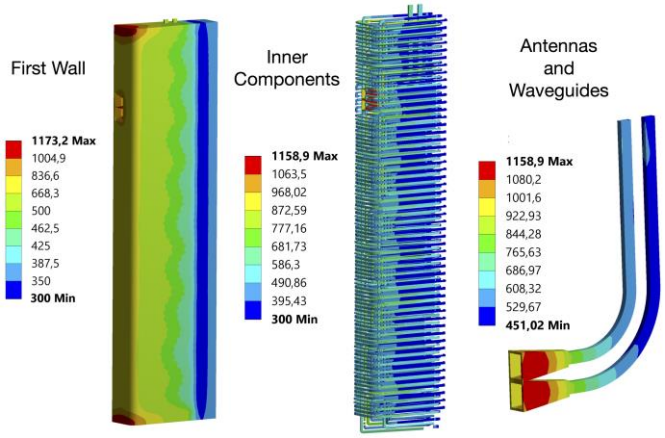

Fig. 15. Operation temperatures in the first wall, cooling system, antennas and waveguides using the boundary conditions defined in section II.

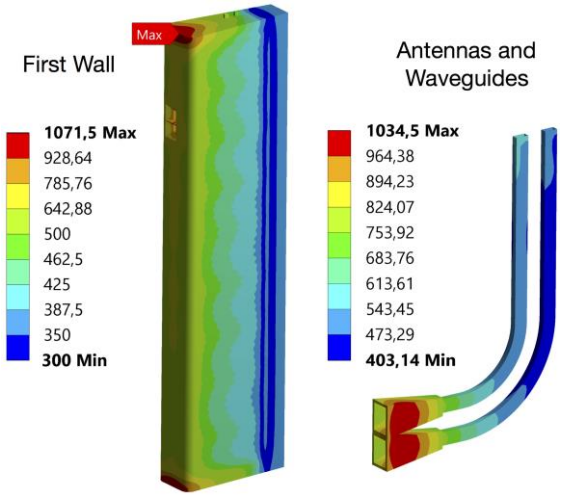

Fig. 16. Operation temperatures in the first wall, cooling system, antennas and waveguides, with the flow of helium in the cooling system increased by 50%.

IV. Conclusions

In this work, we presented a first design of an innovative concept for the integration of several groups of antennas and waveguides into a full poloidal section of the DEMO HCLL breading blankets, dedicated to reflectometry. One of the modules of this Slim Cassette was studied in detail, and a preliminary design of its cooling system was developed. Nuclear and thermal analyses were performed for this model, using MCNP6 and ANSYS Mechanical. Results show that the direct exposure to intense neutron and photon fluxes, as well as to the thermal radiation coming from the plasma, creates hotspots in the proposed design, mostly in regions located further away from the cooling channels, such as the antennas and some parts of the first wall. Apart from these hotspots, it is

shown that with an adequate routing of the cooling system it is possible to lower the operation temperatures to acceptable values, even in the most exposed areas of the first wall. Future iterations will aim at improving the design of the cooling system to increase the flow of helium in the identified hotspots.

ACKNOWLEDGMENT

This work has been carried out within the framework of the EUROfusion Consortium and has received funding from the Euratom research and training programme 2014-2018 under grant agreement No. 633053. The reviews and opinions expressed herein do not necessarily reflect those of the European Commission.

REFERENCES

[1] *CATIA® V5,* Dassault Systèmes*,* Release 6R2016

[2] A*NSYS® Academic Associate,* Release 18.0

[3] Y. Li et al. *"Benchmarking of MCAM 4.0 with the ITER 3D model"*, Fus. Eng. Des. 82 (2007) 2861–2866

[4] Y. Wu, FDS Team, *"CAD-based Interface Programs for Fusion Neutron Transport Simulation"*, Fus. Eng. Des. 84 (2009) 1987-1992

[5] G. W. McKinney, F. B. Brown, et al, *"MCNP 6.1.1 New Features Demonstrated"*, IEEE 2014 Nuclear Science Symposium, Seattle, Nov 8-15, LA-UR-14-23108 (2014)

[6] U. Fischer, *"PMI-3.3-T014-D001 - Guidelines for neutronic analyses 2L8TR9 v1.5"* (2016)

[7] F. Incropera et al. *"Principles of Heat and Mass Transfer"*, 7th Edition, John Wiley & Sons Singapore Pte. Ltd., 2013, p. 544.